ACS OMEGA

http://pubs.acs.org/journal/acsodf

Article

# Robust Design of a Dimethyl Ether Production Process Using Process Simulation and Robust Bayesian Optimization

Yuki Nakayama and Hiromasa Kaneko*

Cite This: *ACS Omega* 2023, 8, 29161−29168

Read Online

ACCESS | Metrics & More | Article Recommendations | Supporting Information

**ABSTRACT:** As greenhouse gases such as $CO_2$ continue to promote global warming, the reduction of $CO_2$ emissions is attracting increasing attention. In this study, we design a process for producing dimethyl ether (DME), which is a promising means of using $CO_2$ as a resource. Design variables such as temperature and pressure need to be optimized to reduce $CO_2$ emissions while maintaining high product purity and DME production. Conventional process designs determine these design variables from the chemical background and through trial-and-error simulations, which are very time-consuming. The proposed method optimizes the design variables efficiently by repeating the process simulations and selecting promising candidates for the design variables using machine learning. For an adaptive design of experiments, Bayesian optimization is used to achieve the objectives of the DME process while efficiently optimizing the design variables. In addition, we also optimize the design variables considering variations in the temperature and pressure data, meaning robust Bayesian optimization. The proposed method successfully identifies design variables that satisfy all experimental targets in an average of 54 simulations while achieving 100% of the targets with product purity 0.95−1.00, amount of DME in the product 350−845 kmol/h, and $CO_2$ emissions 0−835 kmol/h, confirming the effectiveness of the proposed robust Bayesian optimization method.

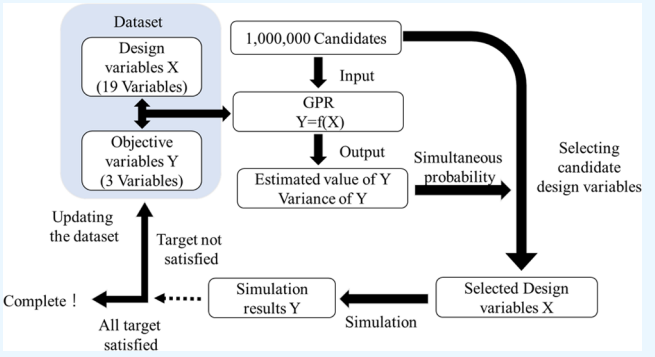


## 1. INTRODUCTION

As the problem of global warming, caused by greenhouse gases such as $CO_2$, becomes more serious, the reduction of $CO_2$ emissions is attracting increasing attention.[1,2] One approach is the development and introduction of renewable energy sources, and a second possibility is the separation and utilization of the $CO_2$ emitted from power plants. The synthesis of dimethyl ether (DME) via methanol is a promising synthetic route whereby $CO_2$ is used as a resource.[3,4] DME can be generated from a wide range of raw materials, including fossil resources such as petroleum, natural gas, and coal, as well as renewable raw materials such as biomass.[5−7]

In recent years, DME has attracted attention as an alternative fuel for household use and diesel engines.[8−10] Various studies have attempted to improve the production capacity of methanol and DME. Otalvaro et al. performed kinetic modeling, model-based optimization, and experimental validation for the direct synthesis of DME from $CO_2$-rich syngas. They used the nonlinear Interior Point OPTimizer solver to optimize the temperature and composition of the catalyst bed and succeeded in increasing the carbon conversion and DME yield. Askari et al. developed a dynamic modeling and optimization method for an autothermal dual-type methanol synthesis unit in the presence of catalyst deactivation. By optimizing the length ratio and feed temperature of the reactor, the methanol production capacity was increased by 5.8% compared with a conventional single reactor.[11] Masoudi et al. succeeded in increasing the methanol production capacity by 6.45% over a conventional dual-type reactor through the dynamic modeling of a dual-type methanol synthesis section. They considered catalyst deactivation and optimization of the feed temperature, cooling water temperature, and other factors to manage the heat.[12] Pérez-Fortes et al. developed a technology for converting $CO_2$ to DME through the three-stage reformation of methane, a low-cost feedstock, with a DME synthesis unit.[13]

In this study, we design a DME production process using $CO_2$ as a raw material. In process design, simulation software is used to determine the design variables.[14] Although the design variables can be determined from the chemical background and through trial-and-error process simulations, as in conventional process designs, it takes a lot of time to optimize the process as the number of design variables increases. Thus,

**Received:** April 7, 2023
**Accepted:** July 27, 2023
**Published:** August 4, 2023





https://doi.org/10.1021/acsomega.3c02344
*ACS Omega* 2023, 8, 29161−29168

there is a need to improve the efficiency of optimizing the design variables.

The objective of this study is to design a DME production process with low environmental impact. To optimize the design variables efficiently, we use machine learning. Askari et al. and Masoudi et al. applied a genetic algorithm to a methanol synthesis section and improved the methanol production capacity.[11,12] Omata et al. combined a genetic algorithm with a neural network to optimize the temperature profile of a temperature gradient reactor, thus improving the conversion of CO under low-pressure conditions.[15] Previous studies have optimized the design variables for certain subprocesses, but the entire process has not been considered in the optimization. We optimize the design variables of the entire process using machine learning, resulting in an efficient DME production process.

To create an adaptive design of experiments, Bayesian optimization (BO),[16,17] which is based on Gaussian process regression (GPR)[18−20] and uses not only predicted $y$ values but also their standard deviations to find candidates for the next experiments, was proposed. The GPR model $Y = f(X)$ is constructed between the design variables $X$ and the objective variables $Y$. Based on predicted $Y$ values and their standard deviations, acquisition functions such as the probability of improvement, expected improvement,[21] mutual information,[22] and probability in target range (PTR)[23] are calculated, and the $X$ candidates with the highest values of the functions are selected. BO allows us to properly search not only for interpolation of existing data sets but also for extrapolation regions, thus reducing the possibility of falling into local optimal solutions. BO has been applied to process simulation,[23] molecular simulation,[24−27] and live experimental optimization.[28−30]

In this study, BO is used to achieve the objectives of the DME process while efficiently optimizing the design variables, and we develop a robust optimization method by considering not only the candidate design conditions but also the surrounding simulation results in the BO acquisition function, which is proposed as robust BO.

The effectiveness of the model is verified by comparing the number of simulations required to achieve the objective with BO and with randomly selected design variables. We also confirm that the design variables can be optimized efficiently in the event of changes in the initial samples.

The main contributions of this study can be summarized as follows.

- The DME process with both low $CO_2$ emission and high product purity and DME production can be automatically and efficiently designed with a small number of process simulations by using Bayesian optimization.
- The proposed robust Bayesian optimization can design variables with variations in the variables around the optimized candidate by considering not only candidates of the variables but also the surrounding simulation results.

## 2. METHODS

**2.1. Process Summary.** A schematic diagram of DME production and related processes is shown in Figure 1. These processes cover the power plant, the $CO_2$ purification process, and the DME production process. The power plant generates electricity using natural gas (NG: $CH_4$, 100%) as fuel. The flue gas emitted by the power plant is sent to the $CO_2$ purification process. In addition to $CO_2$, $N_2$ is present in the flue gas emitted by the power plant. To use $CO_2$ as a raw material, it is necessary to separate and recover the $CO_2$ from the flue gas.

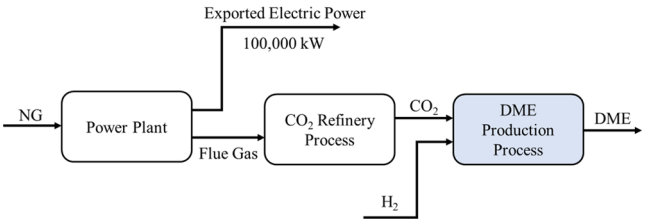


**Figure 1.** Schematic diagram of the DME production process and related processes.

In the $CO_2$ refinery process, $CO_2$ is separated and recovered from the flue gas using a Benfield solution.[31] The flue gas is cooled by a water scrubber, pressurized by a compressor, and fed to the Benfield process. The $CO_2$ in the flue gas is absorbed by the Benfield fluid, and the off-gas, which is mainly composed of nitrogen, is released to the atmosphere after energy recovery in the flue gas turbine because of its high pressure. The absorbed $CO_2$ is dissipated under nearly atmospheric pressure and sent to the DME production process. The refined $CO_2$ is sent to the DME production process, whereby DME is produced via methanol. The $CO_2$ emitted by the power plant for the generation of electricity, which is sold externally, is used as the raw material. The process of synthesizing DME also requires power from compressors and pumps, which is supplied by the power plant. In other words, in addition to the $CO_2$ emissions required for power generation, the power plant emits additional $CO_2$ to supply the electricity and utility steam required for $CO_2$ purification and DME production. In this study, a DME production process is designed, in which the $CO_2$ emitted to produce 100,000 kW electricity and the $CO_2$ emissions from the $CO_2$ purification process (854.55 kmol/h) are less than the feedstock $CO_2$ (1689.93 kmol/h). The DME production process needs to produce DME with $CO_2$ emissions of 835.38 kmol/h or less.

The $CO_2$ reduction per unit DME production can be calculated using the following formula.

$$\text{CO}_2\text{ reduction per unit DME production} = \frac{1689.93 - \text{CO}_2\text{ emissions in the DME production process}}{\text{DME production}} \quad (1)$$

A block flow diagram of the designed DME production process is shown in Figure 2. In the feedstock boosting section, the pressure of the feedstock $CO_2$ and $H_2$ is enhanced by repeatedly boosting the pressure using a compressor and then cooling the feedstock using cooling water. In the methanol synthesis section, the raw materials mixed in the feedstock boosting section are heated to the reaction temperature using a heat exchanger with utility steam, and then, methanol is synthesized in the methanol reactor. The outlet gas of the methanol reactor contains a large amount of $H_2$, $CH_4$, and $CO_2$ in addition to the synthesized methanol. In the gas−liquid separation and recycling section, the superheated gas at the outlet of the methanol reactor is depressurized by an expander, cooled by a heat exchanger using cooling water, and then separated into gas and liquid components. The gas separated


https://doi.org/10.1021/acsomega.3c02344
ACS Omega 2023, 8, 29161−29168

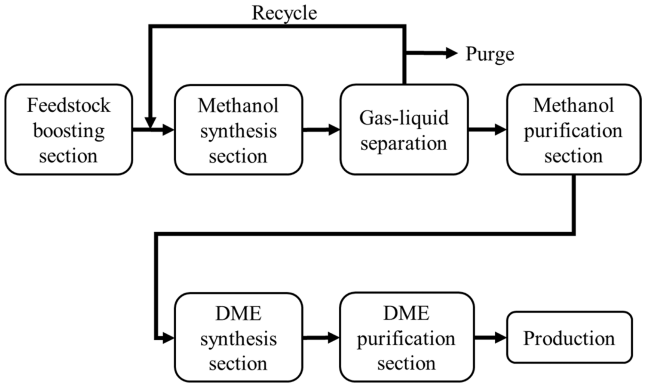


**Figure 2.** Block flow diagram of the designed DME production process.

by gas−liquid separation is partially purged to recycle the $CH_4$ contained in the raw material without concentrating it. The gas that is not purged is pressurized by a compressor and mixed with the $CO_2$ and $H_2$ for recycling. In the methanol purification section, the liquid separated by gas−liquid separation is depressurized by a valve, and then, $H_2O$ and methanol are separated in a distillation column. The $H_2O$ is discharged as liquid from the bottom of the column, and the methanol is discharged as gas from the top of the column. In addition, the remaining material has its pressure increased by a compressor and is then cooled by cooling water, before the methanol and impurities such as $CO_2$ and CO that could not be separated by gas−liquid separation are separated in a distillation column. The methanol is discharged as a liquid from the bottom of the column.

In the DME synthesis section, the methanol obtained from the methanol purification section is pressurized by a pump, and the temperature is raised to the reaction temperature using the product (high-temperature fluid) discharged from the DME reactor and utility steam. In the DME reactor, DME is synthesized from methanol. In the DME purification section, the DME synthesized in the DME reactor is separated from $H_2O$ in a distillation column. The $H_2O$ is discharged from the bottom of the column as liquid, and the DME is discharged from the top of the column as gas. The process flow diagram of the designed DME production process is shown in Figure S1.

**2.2. Reaction Equation and Reaction Kinetics Equation.** In the DME production process considered in this study, DME is produced through a two-step reaction process. The first reaction step is the methanol reaction step, which involves the following two reactions.

$$CO_2(g) + 3H_2(g) \rightleftarrows CH_3OH(g) + H_2O(g) \quad (2)$$

$$CO_2(g) + H_2(g) \rightleftarrows CO(g) + H_2O(g) \quad (3)$$

Equation 2 describes the synthesis reaction of methanol from $CO_2$, which is an exothermic reaction. Equation 3 describes the reverse aqueous gas shift reaction, which is endothermic.

The second step of the reaction process involves the following synthesis reaction of DME from methanol.

$$2CH_3OH(g) \rightleftarrows CH_3OCH_3(DME)(g) + H_2O(g) \quad (4)$$

The kinetic equations for each reaction are as follows.

$$r_1 = 6.5734 \times 10^{-6} \cdot \exp\left(-\frac{36\,696}{RT}\right) \cdot \frac{\left[p_{CO_2}p_{H_2} - \frac{1}{K_{E1}}\left(\frac{p_{MeOH}p_{H_2O}}{p_{H_2}^2}\right)\right]}{\left[1 + 3453.38\left(\frac{p_{H_2O}}{p_{H_2}}\right)\right]^3} \quad (5)$$

$$K_{E1} = \exp(-47.777962 + 7057.7258/T) \quad (6)$$

$$r_2 = 7.49487 \times 10^{6} \cdot \exp\left(-\frac{94\,765}{RT}\right) \cdot \frac{\left[p_{CO_2} - \frac{1}{K_{E2}}\left(\frac{p_{CO}p_{H_2O}}{p_{H_2}}\right)\right]}{\left[1 + 3453.38\left(\frac{p_{H_2O}}{p_{H_2}}\right)\right]} \quad (7)$$

$$K_{E2} = \exp(4.67192 - 4773.2589/T) \quad (8)$$

$$r_3 = k_3[p_{MeOH} - (p_{DME}p_{H_2O})/(p_{MeOH}K_{E3})] \quad (9)$$

$$\ln(k_3) = -1.7954 - 9680/T \quad (10)$$

$$\ln(K_{E3}) = -2.8086 + 3061/T \quad (11)$$

where $r_i$ is the reaction rate constant in equation $(i)$, $p_i$ is the pressure of component $i$, $R$ is the gas constant, and $T$ is the temperature.

**2.3. Creating the Initial Data Set.** In machine learning, a regression model of the form $Y = f(X)$ is constructed between the design variables $X$ and the objective variables $Y$ using a data set. Because there is no data set including $Y$ values or simulation results for the reaction considered in this study, we design the experiments based on the D-optimality criterion.[32] In the design of experiments, candidates of $X$ are selected such that a good model $Y = f(X)$ can be constructed. The task of preparing the initial data set is illustrated in Figure 3. First,

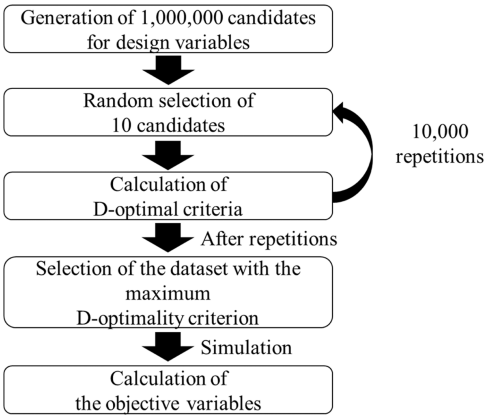


**Figure 3.** Initial data-set creation.

1,000,000 candidates of $X$ are randomly generated. Second, the process of randomly selecting 10 samples out of these 1,000,000 candidates is repeated 10,000 times, and the 10 samples with the maximum D-optimality criterion are selected (in this study, the number of samples in the initial data set is set to 10). The Y values are then calculated by conducting simulations using the selected candidates of $X$. This completes the preparation of the initial data set.



https://doi.org/10.1021/acsomega.3c02344
ACS Omega 2023, 8, 29161−29168

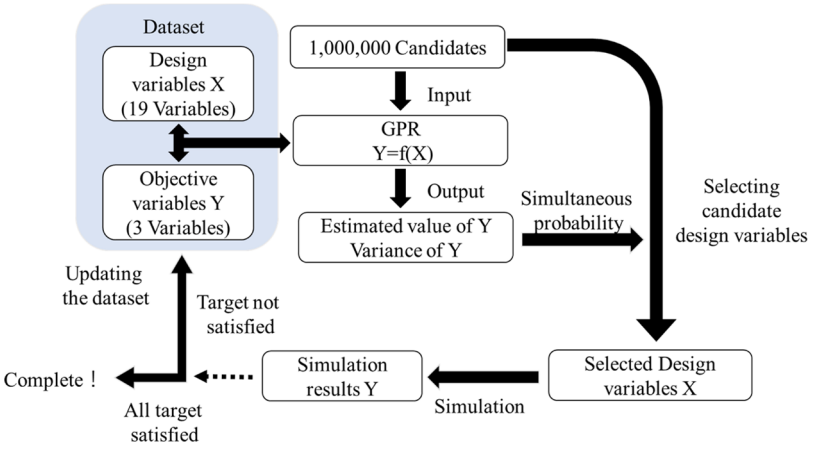


**Figure 4.** Flow of the adaptive design of experiments.

**2.4. Optimization Method.** An adaptive design of experiments based on BO is used to optimize the design variables. The flow of the adaptive design of experiments is shown in Figure 4. The regression model $Y = f(X)$ is constructed by GPR between the design variables $X$ (see Table 1) and the objective variables $Y$ (see Table 2). GPR can be used for both linear and nonlinear regressions. One of its major features is that it calculates both the estimated value and variance of $Y$, allowing us to consider the variability of the estimated value. We input the 1,000,000 candidate design variables generated when creating the initial data set into the constructed model $Y = f(X)$ and calculate the estimated value and variance of $Y$. From the estimated value and variance of $Y$, we calculate the value of the acquisition function. In this study, we use the PTR as the acquisition function—this is the probability that the predicted value of $Y$ will fall within a set target range. In this analysis, we set three objective variables: product purity, amount of DME in the product, and $CO_2$ emissions. We set a target range for each of these objectives. Note that when probabilities are multiplied together, the result is the probability that the individual events will occur simultaneously (i.e., simultaneous probability). In this study, the PTR of each objective variable is calculated, and then a logarithmic transformation is applied to the values. The sum of these transformed values is used as the simultaneous probability. Next, the candidate with the largest simultaneous probability is selected and simulated. If all of the simulation results are within the target range, the BO process is complete. If even one of the simulation results does not fall within the target range, new candidate design variables and results are added to the data set. The operation described above is then repeated using the updated data set.

**Table 1. Design Variables**

| variable number | variable name | equipment name | units | min | max |
|---|---|---|---|---|---|
| X01 | compressor outlet pressure | K6 | bar | 20.00 | 65.00 |
| X02 | hydrogen flow rate | SRC2 | kmol/h | 3000.0 | 10000 |
| X03 | methanol reactor temperature | R1 | °C | 200.0 | 260.0 |
| X04 | purge ratio | SP1 | | 0.001 | 0.060 |
| X05 | valve outlet pressure | XV1 | bar | 0.50 | 1.50 |
| X06 | number of distillation column stages | C1 | | 12 | 14 |
| X07 | distillation column feed stage | C1 | | 2 | 4 |
| X08 | distillation column reflux ratio | C1 | | 0.100 | 2.000 |
| X09 | compressor outlet pressure | K8 | bar | 1.50 | 2.10 |
| X10 | number of distillation column stages | C2 | | 9 | 11 |
| X11 | distillation column feed stage | C2 | | 1 | 3 |
| X12 | distillation column reflux ratio | C2 | | 0.100 | 1.500 |
| X13 | condenser outlet temperature | E11 | °C | 30.0 | 50.0 |
| X14 | pump outlet pressure | P1 | bar | 10.00 | 15.00 |
| X15 | DME reactor temperature | R2 | °C | 250.0 | 380.0 |
| X16 | number of distillation column stages | C3 | | 12 | 14 |
| X17 | distillation column feed stage | C3 | | 6 | 8 |
| X18 | distillation column reflux ratio | C3 | | 0.100 | 1.000 |
| X19 | condenser outlet temperature | E14 | °C | 45.0 | 55.0 |

**Table 2. Objective Variables**

| variable number | variable name | units | min | max |
|---|---|---|---|---|
| Y01 | product purity | | 0.95 | 1.00 |
| Y02 | amount of DME in the product | kmol/h | 350 | 845 |
| Y03 | $CO_2$ emissions | kmol/h | 0 | 835 |

**2.5. Robust Bayesian Optimization under Variations in Design Variables.** Design variables such as temperature and pressure do not remain constant but fluctuate continuously. We optimize the design variables to account for such temperature and pressure variations. The optimization process is described below. Most of the process is the same as for the adaptive design of experiments based on BO, as shown in Figure 4. A regression model between the design variables $X$ and the objective variables Y is constructed using GPR. The 1,000,000 candidate design variables generated for the initial data set are input into the constructed model $Y = f(X)$, and the estimated value and variance of $Y$ are obtained. The PTR values are then calculated. The next step is to select the candidate design variables that have the highest PTR values. Based on the design variable candidates selected here, 10 new design variable candidates are generated within a range of ±3%



https://doi.org/10.1021/acsomega.3c02344
ACS Omega 2023, 8, 29161−29168

for each design variable. For example, if the temperature of the base design variable is 50 °C, the newly generated temperature candidates will be in the range [48.5, 51.5 °C].

Because the numbers of distillation column stages and feed stages do not vary, they provide the candidate design variables. As shown in Figure 5, simulations are performed with the new

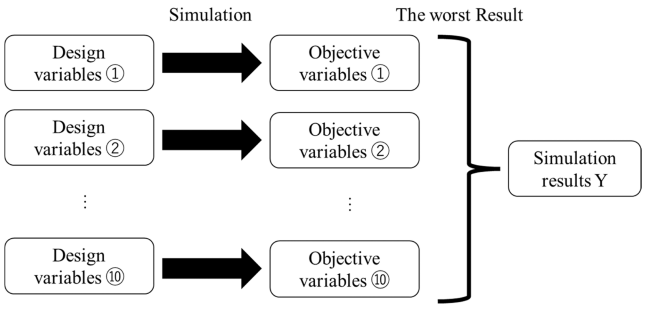


**Figure 5.** Robust Bayesian optimization for variations in design variables.

candidate design variables, and the worst result is treated as the actual value of the objective variables. This makes it possible to search for a solution that is not affected by small changes in the design variables. If the values of all of the objective variables are within the target range, the BO process is considered complete. If even a single objective variable does not fall within the target range, the candidate design variables and results are added to the data set. The operation described above is then repeated using the updated data set.

## 3. RESULTS AND DISCUSSION

**3.1. Optimization of Design Variables Based on Adaptive Design of Experiments.** The adaptive design of experiments based on BO was used to optimize the design variables. To verify the effectiveness of BO, we also randomly selected the design variable candidates. We performed BO 3 times with different initial samples and performed random selection 3 times as well. An example of the three trials is shown below. Figures 6 and 7 show examples of the optimization results for BO and random selection, respectively. The horizontal axis is the number of simulations, and the vertical axis is the value of the objective variable. The orange region is the target range. As shown for the last sample in Figure 6, all of the objective variables are within the target range. By using adaptive design of experiments based on BO, we were able to find the design variables that satisfy the target range for product purity, amount of DME in the product, and $CO_2$ emissions after 48 simulations out of 1,000,000 candidates. The product purity was found to be 0.962, the amount of DME in the product was 512.43 kmol/h, and the $CO_2$ emissions were 800.10 kmol/h. In the case of random selection, Figure 7 shows that in some simulations certain objective variables were in the target range, but there was no simulation result in which all three objective variables were in the target range at the same time. Even after 100 iterations of randomly selecting design variables from 1,000,000 candidates, we could not find design variables that satisfied the target ranges of all three objective variables.

In the three verifications, BO was able to find design variables that satisfied the target ranges of all three objective variables in 48, 31, and 54 simulations, separately. In contrast, random selection was not able to find design variables that satisfied all of the target ranges after 110 simulations, the maximum number of simulations permitted in the verifications. The values of each objective variable and the number of simulations are presented in Table 3, and the values of the design variables optimized by BO are listed in Table 4. The methanol reactor temperature (X03) is 202.1 °C, which is close to the lower limit of 200 °C. By using the adaptive design of experiments based on BO, it was possible to find design variables that satisfied all target ranges after an average of 44.3 simulations from among 1,000,000 candidates. In the case of randomly selected design variable candidates, it was not possible to find design variables that satisfied all of the targets after 110 simulations, suggesting that the adaptive design of experiments based on BO is an effective method for efficiently optimizing design variables. Even when the initial samples changed, the number of simulations did not increase significantly, indicating that the adaptive design of experiments based on BO is robust.

**3.2. Optimization Accounting for Variations in Design Variables.** As shown in Figure 8, we were able to find design variables that satisfy the target ranges for product purity, DME content, and $CO_2$ emissions after 54 simulations from among 1,000,000 candidates. The product purity was

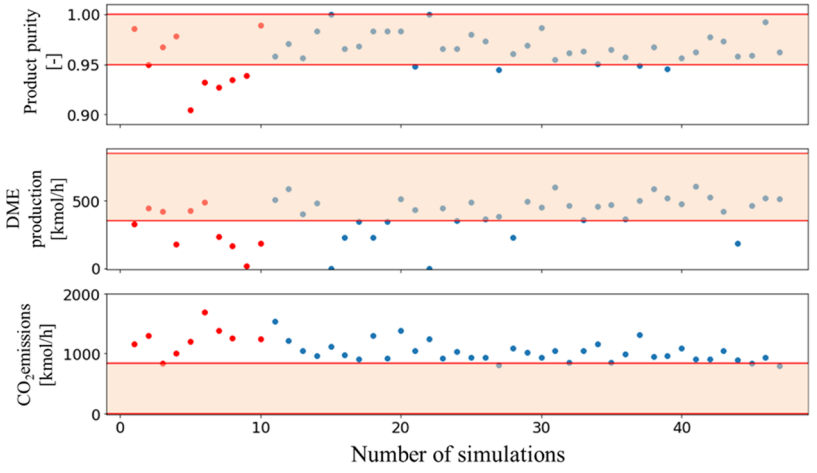


**Figure 6.** Result example of BO. Red points are the objective variable values for the initial 10 samples, blue points are the objective variable values during BO, and orange areas are the target ranges.



https://doi.org/10.1021/acsomega.3c02344
ACS Omega 2023, 8, 29161−29168

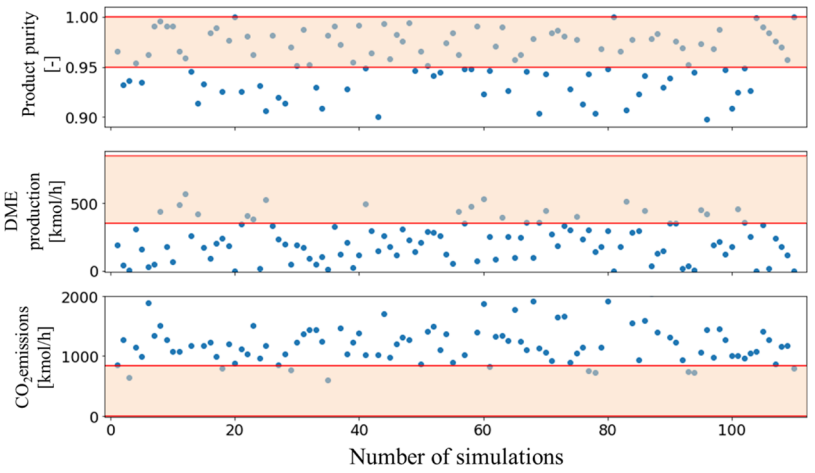


**Figure 7.** Result example of random selection. Blue points are the objective variable values. Orange areas are the target ranges.

**Table 3. Comparison of BO and Random Selection**

| method | product purity [-] | DME in the product [kmol/h] | $CO_2$ emissions [kmol/h] | number of simulations | average |
|---|---|---|---|---|---|
| BO ① | 0.962 | 512.43 | 800.10 | 48 | 44.3 |
| BO ② | 0.963 | 437.70 | 773.60 | 31 | |
| BO ③ | 0.970 | 354.20 | 834.71 | 54 | |
| Random ① | | | | 110 (fail) | 110 (fail) |
| Random ② | | | | 110 (fail) | |
| Random ③ | | | | 110 (fail) | |

0.969, the amount of DME in the product was 361.79 kmol/h, and the $CO_2$ emission was 832.93 kmol/h. Even in the event of variations in temperature and pressure, it was possible to identify design variables that would satisfy all of the target ranges. The $CO_2$ reduction per unit DME production was 2.37 [-] from eq 1. The optimized design variables are listed in Table 5. The methanol reactor temperature (X03) is 202.1 °C, which is close to the lower limit of 200 °C. Low temperature and high pressure are advantageous for the synthesis of methanol from $CO_2$,[33] which is consistent with the results of this study.

## 4. CONCLUSIONS

An adaptive design of experiments based on BO has been developed to find design variables that satisfy the target ranges for product purity, amount of DME in the product, and $CO_2$ emissions. The proposed method successfully identified design variables that satisfied all targets in an average of 44.3 simulations. In comparison, a random search method could not find design variables that would satisfy all of the target ranges in 110 simulations. This result confirms the effectiveness of the optimization method.

We also conducted the optimization process considering variation in certain design variables. By using the adaptive design of experiments, we could identify design variables that simultaneously achieved all of the targets in an average of 54 simulations. Because the proposed method can be applied to any process design, it is expected to achieve efficiency improvements in a range of industrial settings.

**Table 4. Optimized Design Parameters**

| variable number | variable name | equipment name | unit | BO1 | BO2 | BO3 |
|---|---|---|---|---|---|---|
| X01 | compressor outlet pressure | K6 | bar | 45.78 | 63.85 | 34.02 |
| X02 | hydrogen flow rate | SRC2 | kmol/h | 6415.4 | 7305.4 | 8455.3 |
| X03 | methanol reactor temperature | R1 | °C | 201.9 | 209.7 | 202.2 |
| X04 | purge ratio | SP1 | | 0.006 | 0.020 | 0.055 |
| X05 | valve outlet pressure | XV1 | bar | 1.42 | 1.41 | 0.55 |
| X06 | number of distillation column stages | C1 | | 12 | 12 | 13 |
| X07 | distillation column feed stage | C1 | | 4 | 3 | 3 |
| X08 | distillation column reflux ratio | C1 | | 1.859 | 1.114 | 0.818 |
| X09 | compressor outlet pressure | K8 | bar | 1.96 | 1.94 | 1.54 |
| X10 | number of distillation column stages | C2 | | 11 | 10 | 11 |
| X11 | distillation column feed stage | C2 | | 1 | 1 | 3 |
| X12 | distillation column reflux ratio | C2 | | 0.396 | 0.195 | 0.416 |
| X13 | condenser outlet temperature | E11 | °C | 43.5 | 30.5 | 31.7 |
| X14 | pump outlet pressure | P1 | bar | 11.98 | 12.69 | 14.30 |
| X15 | DME reactor temperature | R2 | °C | 251.6 | 250.0 | 270.5 |
| X16 | number of distillation column stages | C3 | | 12 | 14 | 14 |
| X17 | distillation column feed stage | C3 | | 8 | 6 | 7 |
| X18 | distillation column reflux ratio | C3 | | 0.184 | 0.500 | 0.773 |
| X19 | condenser outlet temperature | E14 | °C | 47.3 | 49.9 | 54.1 |



https://doi.org/10.1021/acsomega.3c02344
ACS Omega 2023, 8, 29161−29168

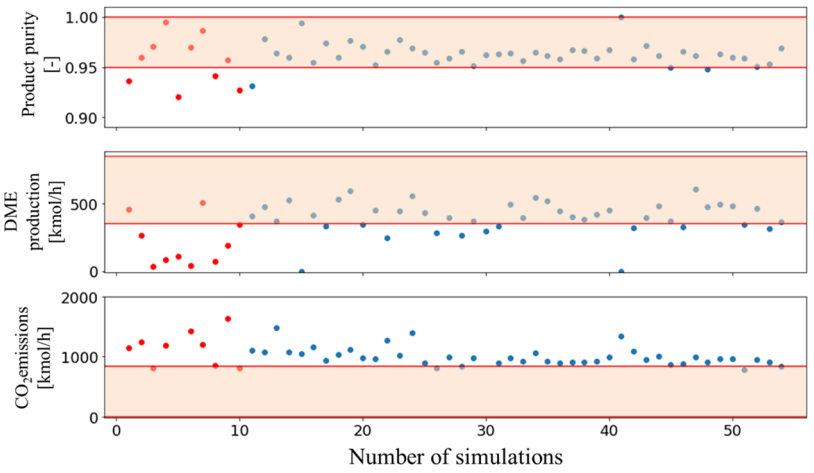


**Figure 8.** Result of optimization of objective variables considering variability of design variables. Red points are the objective variable values for the initial 10 samples, blue points are the objective variable values during BO, and orange areas are the target ranges.

**Table 5. Optimization of Design Variables Considering Variability**

| variable number | design variable name | equipment name | unit | optimization |
|---|---|---|---|---|
| X01 | compressor outlet pressure | K6 | bar | 51.04 |
| X02 | hydrogen flow rate | SRC2 | kmol/h | 9442.1 |
| X03 | methanol reactor temperature | R1 | °C | 202.1 |
| X04 | purge ratio | SP1 | | 0.046 |
| X05 | valve outlet pressure | XV1 | bar | 1.34 |
| X06 | number of distillation column stages | C1 | | 14 |
| X07 | distillation column feed stage | C1 | | 3 |
| X08 | distillation column reflux ratio | C1 | | 0.909 |
| X09 | compressor outlet pressure | K8 | bar | 1.63 |
| X10 | number of distillation column stages | C2 | | 9 |
| X11 | distillation column feed stage | C2 | | 2 |
| X12 | distillation column reflux ratio | C2 | | 0.223 |
| X13 | condenser outlet temperature | E11 | °C | 35.6 |
| X14 | pump outlet pressure | P1 | bar | 13.15 |
| X15 | DME reactor temperature | R2 | °C | 322.1 |
| X16 | number of distillation column stages | C3 | | 14 |
| X17 | distillation column feed stage | C3 | | 8 |
| X18 | distillation column reflux ratio | C3 | | 0.373 |
| X19 | condenser outlet temperature | E14 | °C | 49.2 |

## ■ ASSOCIATED CONTENT

### Data Availability Statement

The software that supports the findings of this study is available at https://github.com/hkaneko1985/dcekit.

### Supporting Information

The Supporting Information is available free of charge at https://pubs.acs.org/doi/10.1021/acsomega.3c02344.

Process flow diagram of the designed DME production process (Figure S1) (PDF)

## ■ AUTHOR INFORMATION


### Corresponding Author

**Hiromasa Kaneko** − *Department of Applied Chemistry, School of Science and Technology, Meiji University, Kawasaki, Kanagawa 214-8571, Japan*; orcid.org/0000-0001-8367-6476; Phone: +81-44-934-7197; Email: hkaneko@meiji.ac.jp

### Author

**Yuki Nakayama** − *Department of Applied Chemistry, School of Science and Technology, Meiji University, Kawasaki, Kanagawa 214-8571, Japan*

Complete contact information is available at: https://pubs.acs.org/10.1021/acsomega.3c02344


### Notes

The authors declare no competing financial interest.

## ■ ACKNOWLEDGMENTS

This study was financially supported by a Grant-in-Aid for Scientific Research (KAKENHI) with grant number 19K15352 from the Japan Society for the Promotion of Science. The authors thank Stuart Jenkinson, PhD, from Edanz (https://jp.edanz.com/ac) for editing a draft of this manuscript.

## ■ REFERENCES

(1) Saravanan, A.; Kumar, P. S.; Vo, D.-V. N.; Jeevanantham, S.; Bhuvaneswari, V.; Narayanan, V. A.; Yaashikaa, P. R.; Swetha, S.; Reshma, B. A comprehensive review on different approaches for CO2 utilization and conversion pathways. *Chem. Eng. Sci.* **2021**, *236*, No. 116515.

(2) Al-Breiki, M.; Bicer, Y. Comparative life cycle assessment of sustainable energy carriers including production, storage, overseas transport and utilization. *J. Cleaner Prod.* **2021**, *279*, No. 123481.

(3) Bahadori, F.; Oshnuie, M. N. Exergy analysis of indirect dimethyl ether production process. *Sustainable Energy Technol. Assess.* **2019**, *31*, 142−145.

(4) Kansha, Y.; Ishizuka, M.; Song, C.; Tsutsumi, A. An Innovative Dimethyl Ether (DME) Production Using Self-Heat Recuperation. *Chem. Eng. Trans.* **2014**, *39*, 109−114.

(5) Giuliano, A.; Catizzone, E.; Freda, C. Process Simulation and Environmental Aspects of Dimethyl Ether Production from Digestate-Derived Syngas. *Int. J. Environ. Res. Public Health* **2021**, *18*, No. 807.
(6) Peral, E.; Martín, M. Optimal Production of Dimethyl Ether from Switchgrass-Based Syngas via Direct Synthesis. *Ind. Eng. Chem. Res.* **2015**, *54*, 7465−7475.
(7) Otalvaro, N. D.; Kaiser, M.; Delgado, K. H.; Wild, S.; Sauer, J.; Freund, H. Optimization of the direct synthesis of dimethyl ether from CO2 rich synthesis gas: closing the loop between experimental investigations and model-based reactor design. *React. Chem. Eng.* **2020**, *5*, 949−960.
(8) Bai, Z.; Ma, H.; Zhang, H.; Ying, W.; Fang, D. Process simulation of dimethyl ether synthesis via methanol vapor phase dehydration. *Pol. J. Chem. Technol.* **2013**, *15*, 122−127.
(9) Shen, W.-J.; Jun, K.-W.; Choi, H.-S.; Lee, K.-W. Thermodynamic Investigation of Methanol and Dimethyl Ether Synthesis from CO2 Hydrogenation. *Korean J. Chem. Eng.* **2000**, *17*, 210−216.
(10) Olah, G. A.; Goeppert, A.; Prakash, G. K. S. Chemical Recycling of Carbon Dioxide to Methanol and Dimethyl Ether: From Greenhouse Gas to Renewable, Environmentally Carbon Neutral Fuels and Synthetic Hydrocarbons. *J. Org. Chem.* **2009**, *74*, 487−498.
(11) Askari, F.; Rahimpour, M. R.; Jahanmiri, A.; Mostafazadeh, A. K. Dynamic Simulation and Optimization of a Dual-Type Methanol Reactor Using Genetic Algorithms. *Chem. Eng. Technol.* **2008**, *31*, 513−524.
(12) Masoudi, S.; Farsi, M.; Rahimpour, M. R. Dynamic optimization of methanol synthesis section in the dual type configuration to increase methanol production. *Oil Gas Sci. Technol. − Rev. IFP Energies nouvelles* **2019**, *74*, 90−102.
(13) Pérez-Fortes, M.; Schöneberger, J. C.; Boulamanti, A.; Tzimas, E. Methanol synthesis using captured CO2 as raw material: Techno-economic and environmental assessment. *Appl. Energy* **2016**, *161*, 718−732.
(14) https://www.aveva.com/ja-jp/products/process-simulation/. (accessed April 01, 2022).
(15) Omata, K.; Ozaki, T.; Umegaki, T.; Watanabe, Y.; ukui, N.; Yamada, M. Optimization of the Temperature Profile of a Temperature Gradient Reactor for DME Synthesis Using a Simple Genetic Algorithm Assisted by a Neural Network. *Energy Fuels* **2003**, *17*, 836−841.
(16) Shahriari, B.; Swersky, K.; Wang, Z. Y.; Adams, R. P.; de Freitas, N. Taking the Human Out of the Loop: A Review of Bayesian Optimization. *Proc. IEEE* **2016**, *104*, 148−175.
(17) Gramacy, R. B. *Surrogates: Gaussian Process Modeling, Design, and Optimization for the Applied Sciences*; CRC Press, 2020.
(18) Bishop, C. M. *Pattern Recognition and Machine Learning*; Springer: New York, 2006.
(19) Burnaev, E.; Panov, M. Adaptive Design of Experiments Based on Gaussian Processes. *Lect. Notes Comput. Sci.* **2015**, *9047*, 116−125.
(20) Rasmussen, C. E.; Williams, C. K. I. *Gaussian Processes for Machine Learning*; The MIT Press: Cambridge, MA, 2006.
(21) Snoek, J.; Larochelle, H.; Adams, R. P. Practical Bayesian Optimization of Machine Learning Algorithms. In *Advances in Neural Information Processing Systems 25*; Pereira, F.; Burges, C. J. C.; Bottou, L.; Weinberger, K. Q., Eds.; Curran Associates, Inc., 2012; pp 2951−2959.
(22) Contal, E.; Perchet, V.; Vayatis, N. In *Gaussian Process Optimization with Mutual Information*, Proceedings of the 31st International Conference on Machine Learning, 2014.
(23) Iwama, R.; Kaneko, H. Design of Ethylene Oxide Production Process Based on Adaptive Design of Experiments and Bayesian Optimization. *J. Adv. Manuf. Process.* **2021**, *3*, No. e10085.
(24) Jalem, R.; Kanamori, K.; Takeuchi, I.; Nakayama, M.; Yamasaki, H.; Saito, T. Bayesian-Driven First-Principles Calculations for Accelerating Exploration of Fast Ion Conductors for Rechargeable Battery Application. *Sci. Rep.* **2018**, *8*, No. 5845.
(25) Doan, H. A.; Agarwal, G.; Qian, H.; Counihan, M. J.; Rodríguez-López, J.; Moore, J. S.; Assary, R. S. Quantum Chemistry-Informed Active Learning to Accelerate the Design and Discovery of Sustainable Energy Storage Materials. *Chem. Mater.* **2020**, *32*, 6338−6346.
(26) Nakano, K.; Noda, Y.; Tanibata, N.; Takeda, H.; Nakayama, M.; Kobayashi, R.; Takeuchi, I. Exhaustive and Informatics-aided Search for Fast Li-ion Conductor with NASICON-type Structure Using Material Simulation and Bayesian Optimization. *APL Mater.* **2020**, *8*, No. 041112.
(27) Seko, A.; Ishiwata, S. Prediction of Perovskite-related Structures in ACuO3−x (A = Ca, Sr, Ba, Sc, Y, La) Using Density Functional Theory and Bayesian Optimization. *Phys. Rev. B* **2020**, *101*, No. 134101.
(28) Shields, B. J.; Stevens, J.; Li, J.; Parasram, M.; Damani, F.; Alvarado, J. I. M.; Janey, J. M.; Adams, R. P.; Doyle, A. G. Bayesian Reaction Optimization as a Tool for Chemical Synthesis. *Nature* **2021**, *590*, 89−96.
(29) Kaneko, D.; Kaneko, H.; Hayashi, F.; Fukaishi, K.; Yamada, T.; Teshima, K. Process-Informatics-Assisted Preparation of Lithium Titanate Crystals with Various Sizes and Morphologies. *Ind. Eng. Chem. Res.* **2023**, *62*, 511−518.
(30) Morishita, T.; Kaneko, H. Initial Sample Selection in Bayesian Optimization for Combinatorial Optimization of Chemical Compounds. *ACS Omega* **2023**, *8*, 2001−2009.
(31) https://wiki.olisystems.com/wiki/Benfield_process.
(32) de Aguiar, P. F.; Bourguignon, B.; Khots, M. S.; Massart, D. L.; Phan-Than-Luu, R. D-optimal designs. *Chemom. Intell. Lab. Syst.* **1995**, *30*, 199−210.
(33) Jadhav, S. G.; Vaidyaa, P. D.; Bhanage, B. M.; Joshi, J. B. Catalytic carbon dioxide hydrogenation to methanol: A review of recent studies. *Chem. Eng. Res. Des.* **2014**, *9*, 2557−2567.


https://doi.org/10.1021/acsomega.3c02344
*ACS Omega* 2023, 8, 29161−29168